

July 1998
Revised, September 1998
Revised, October 1998

Anatomy of a quantum ‘bounce’

M. A. Doncheski

Department of Physics
The Pennsylvania State University
Mont Alto, PA 17237 USA

and

R. W. Robinett

Department of Physics
The Pennsylvania State University
University Park, PA 16802 USA

Abstract

We discuss some of the properties of the ‘collision’ of a quantum mechanical wave packet with an infinitely high potential barrier, focusing on novel aspects such as the detailed time-dependence of the momentum-space probability density and the time variation of the uncertainty principle product $\Delta x_t \cdot \Delta p_t$. We make explicit use of Gaussian-like wave packets in the analysis, but also comment on other general forms.

I. Introduction

The use of wave packets to analyze the non-trivial time-dependence of quantum mechanical systems is one important aspect of the study of the classical-quantum interface. Popular simulation packages [1] can help students visualize the evolution of quantum states (as opposed to time-independent stationary state solutions [2], [3], [4], [5]) by allowing them to continuously change parameters (such as the initial width of a wave packet) to study what effect they have on the system under study.

A number of authors have considered various one-dimensional quantum mechanical problems in a wave packet approach studying transmission and reflection from square barriers [6], [7], [8], [9] or linear potential steps [10], bound state wave packets in single square wells in either position space [11] or momentum space [12], in double wells [13], [14], or in systems of relevance to solid state physics [15], [16]. Such examples of wave packet behavior are also increasingly useful as teaching tools since the behavior of Coulomb wave packets on circular [17] or elliptical [18] orbits are being tested experimentally on Rydberg atom systems [19], [20].

Numerical methods for solving the time-dependent Schrödinger equation have been discussed [6], [21] and, in special cases, closed-form analytic results can be obtained by use of the time-development operator [22], [23], $e^{-i\hat{H}t/\hbar}\psi(x, 0) = \psi(x, t)$, to solve the initial value problem. Another approach is to combine a large number of individual stationary state solutions for both unbound [24] and bound state problems [11] to obtain wave packets. The most familiar example is the explicit calculation of the Gaussian free-particle wave packet which is treated in the majority of elementary texts.

A simple variation is to consider a particle, subject to the one-dimensional ‘infinite wall’ potential [5] given by

$$V(x) = \begin{cases} 0 & \text{for } x < 0 \\ \infty & \text{for } x \geq 0 \end{cases} \quad (1)$$

so that it is free for $x < 0$, but a wavepacket impinging on the ‘wall’ at the origin will ‘bounce’. Andrews [25] has shown how some of the most obvious aspects of the ‘collision’ process (namely the long-time development of the reflected wave packet, interference effects during the ‘collision’, etc.) can be understood by considering combinations of free-particle ‘mirror’ solutions, and we will use some of his arguments.

In this note we will examine, in some detail, the ‘bounce’ of free-particle wave packets from the infinite wall potential described by Eqn. (1), focusing on several other issues, namely the behavior of the momentum-space wave packet solutions, the widths of the position- and momentum-space packets during the ‘bounce’, and the uncertainty principle product $\Delta x_t \cdot \Delta p_t$ as a function of time. We will make extensive use of the free-particle Gaussian wave packet in our discussion, but we also present results for other, more general forms; for completeness sake, however, we very briefly review the essentials of the Gaussian case.

A free-particle wave packet can be constructed, using any initial momentum-space weighting function, $\phi(p, 0)$, via

$$\psi(x, t) = \frac{1}{2\pi\hbar} \int_{-\infty}^{+\infty} e^{ipx/\hbar} e^{-ip^2t/2m\hbar} \phi(p, 0) dp \quad (2)$$

to give a time-dependent position-space wavefunction, $\psi(x, t)$. The momentum-space solution itself has a trivial time-dependence, namely

$$\phi(p, t) = \phi(p, 0) e^{-ip^2t/2m\hbar} \quad (3)$$

For the case of a Gaussian momentum-distribution, here written in the form

$$\phi_1(p, 0) = \sqrt{\frac{\alpha}{\sqrt{\pi}}} e^{-\alpha^2(p-p_0)^2/2} e^{-ipx_0/\hbar} \quad (4)$$

the necessary integral in Eqn. (2) can be done to obtain the well-known result

$$\psi_1(x, t) = \frac{1}{\sqrt{\alpha\hbar F \sqrt{\pi}}} e^{i[p_0(x-x_0)-p_0^2t/2m]/\hbar} e^{-(x-x_0-p_0t/m)^2/2\alpha^2\hbar^2 F} \quad (5)$$

where $F = 1 + it/t_0$ and $t_0 \equiv m\hbar\alpha^2$. This solution describes a Gaussian position-space wave packet whose width increases with time, characterized by arbitrary initial values of x_0 and p_0 . The resulting position-space probability density is

$$P_{free}(x, t) = |\psi_1(x, t)|^2 = \frac{1}{\beta_t \sqrt{\pi}} e^{-(x-x_0-p_0t/m)^2/\beta_t^2} \quad (6)$$

where $\beta_t \equiv \alpha\hbar[1 + (t/t_0)^2]^{1/2}$ and various important expectation values are given by

$$\langle x \rangle_t = x_0 + \frac{p_0 t}{m} \quad , \quad \Delta x_t = \frac{\alpha\hbar}{2} \sqrt{1 + \left(\frac{t}{t_0}\right)^2} \quad , \quad \langle p \rangle_t = p_0 \quad , \quad \Delta p_t = \frac{1}{\sqrt{2}\alpha} \quad (7)$$

For the infinite wall case, we also can obtain wave packet solutions from Eqn. (2) by substituting the appropriate plane wave solutions

$$e^{ipx/\hbar} \quad \longrightarrow \quad \begin{cases} e^{ipx/\hbar} - e^{-ipx/\hbar} & \text{for } x \leq 0 \\ 0 & \text{for } x \geq 0 \end{cases} \quad (8)$$

in the basic integral. In this approach, the integrals must be performed numerically. On the other hand, we can also make use of the method of Andrews [25] and use *any* free-particle wave packet solution $\psi(x, t)$ via

$$\tilde{\psi}(x, t) = \begin{cases} \psi(x, t) - \psi(-x, t) & \text{for } x \leq 0 \\ 0 & \text{for } x \geq 0 \end{cases} \quad (9)$$

which satisfies the Schrödinger equation for the potential in Eqn. (1) as well as the appropriate boundary condition at the wall. In either case, if the original free-particle

wave packet is properly normalized, the ‘bouncing’ wavepackets will also be very close to being normalized, provided they are initially far enough from the wall so that any contribution from the ‘tail’ in the $x > 0$ region is negligible. In either case, however, in order to obtain the time-dependent momentum-space wavefunction, we must numerically evaluate the Fourier transform

$$\phi(p, t) = \frac{1}{\sqrt{2\pi\hbar}} \int_{-\infty}^{+\infty} e^{-ipx/\hbar} \psi(x, t) dx \quad (10)$$

To illustrate the behavior of such a ‘bouncing’ wave packet, we show in Fig. 1 plots of the position- and momentum-space probability densities for a Gaussian wavepacket for various times before and after a collision. We have used the following values in numerical integrals:

$$\hbar = 1 \quad , \quad m = 1 \quad , \quad p_0 = 10 \quad , \quad x_0 = -10 \quad , \quad \alpha = 1 \quad (11)$$

With these values, the spreading time is $t_0 = 1$ and the time it takes the packet to return to its initial starting point is $T = 2t_0 = 2$, so that an appreciable amount of spreading is obvious. In order to see what features of such ‘collisions’ are specific to Gaussian packets, in Fig. 2 we show the same plots, but for an initial momentum-space amplitude given by a Lorentzian form, namely

$$\phi_2(p, 0) = \sqrt{\frac{2\alpha}{\pi}} \frac{1}{[\tilde{\alpha}^2(p - p_0)^2 + 1]} e^{-ipx_0/\hbar} \quad (12)$$

The corresponding initial position-space wavefunction is

$$\psi_2(x, 0) = \frac{1}{\sqrt{\tilde{\alpha}\hbar}} e^{-|x-x_0|/\tilde{\alpha}\hbar} \quad (13)$$

but the further time-dependence can only be evaluated numerically using Eqn. (2).

Using these two cases, we can make some general comments:

- (i) The non-Gaussian position-space wave packet comes to approach the Gaussian form more and more closely, as it evolves in time. This behavior is seen for a large number of other, single-humped initial distributions [26].
- (ii) The momentum-space probability density well after the collision is related to the initial density by $P_{after}(p, t) = P_{before}(-p, t)$ corresponding to the reversal of each momentum component during to the collision.
- (iii) At the moment of the collision, however, the momentum distribution is *not* symmetric. This is clearly due to the fact that the high momentum components are preferentially in the leading edge, and are the first to be reflected to negative values. This also implies, as will be seen later, that the expectation value $\langle p \rangle_t$ is slightly negative at $t = T_C$, the collision time. We note that other ‘velocity effects’ have been discussed [7], [8] for various kinds of wave packet scattering.

To focus on the details of the collision event, in Fig. 3 we plot the time-dependent $|\psi(x, t)|^2$ and $|\phi(p, t)|^2$ (for the Gaussian wave packet) for times nearer the actual ‘bounce’, bracketing $t = T_C$, and we note some additional aspects of the process:

- (i) The time-dependence of $\phi(p, t)$, which is non-trivial only during the collision, is more clearly visible as is the eventual return to ‘symmetry’ of $|\phi(p, t)|^2$.
- (ii) The spread in the position-space probability density at the time of the collision is substantially smaller than Δx_t either immediately before or after the collision. We will address this point below, using an analytical evaluation of $\Delta x_{t=T_C}$.

In order to examine more of the differences between the purely classical and quantum approaches to the collision of a point particle, we plot in Fig. 4 calculations of

the expectation values $\langle x \rangle_t$ and $\langle p \rangle_t$, which are easily evaluated numerically. In this figure, we show the expectation values of x and p (solid curves) for the bouncing wave packet, as well as those for the free-particle wave packet (dotted curves) for the standard set of parameters in Eqn. (11) except that we use the value of $\alpha = 0.5$; this value is chosen to make the spreading of the wave packets more obvious since in this case $t_0 = m\hbar\alpha^2$ is much smaller. We also indicate the ‘one sigma’ limits given by $\langle x \rangle_t \pm \Delta x_t$ and $\langle p \rangle_t \pm \Delta p_t$ as dashed curves.

We first note that the guaranteed relationship between $\langle x \rangle_t$ and $\langle p \rangle_t$, namely $\langle p \rangle_t = md\langle x \rangle_t/dt$, is trivially observed long before and long after the collision, while the same qualitative connection between $\langle x \rangle_t$ and $\langle p \rangle_t$ near $t = T_C$ is now also apparent and different than a purely classical ‘bounce’ for a point particle which would have a cusp (discontinuity) in $x(t)$ ($v(t)$) at the collision time. Finally, we can see that the position spread at the collision time, $\Delta x_{t=T_C}$ is slightly smaller for the ‘bouncing’ wavepacket than for the free-particle packet with the same initial parameters, while the momentum spread is much larger at T_C than in the free-particle case.

In order to examine the ‘compression’ of $\psi(x, T_C)$ and related issues, we plot in Fig. 5 the values of Δx_t , Δp_t and the uncertainty principle product $\Delta x_t \cdot \Delta p_t$ (in units of \hbar) for a range of values of α , but keeping the other parameters fixed as in Eqn. (11). In each case we see that $\Delta x_{t=T_C}$ is indeed smaller than its value for the free-particle wave packet and in the cases where $\alpha \geq 1$, it is even smaller than its original spread, $\Delta x_{t=0}$. This effect is perhaps intuitively obvious as the high momentum components are reflected first, while the low momentum pieces ‘pile up’, leaving the position-space wave packet temporarily narrower. This is not a violation of the $x - p$ uncertainty principle as many other cases of such behavior are known; for example, similar effects

are seen in explicit constructions of wave packet solutions [27] or more simply in the direct examination of the time-dependence of the uncertainties in x and p in complete generality [28], for the harmonic oscillator potential. In our case, the fact that Δp_t does indeed increase during the collision is even more obvious, especially from the time-dependence of $|\phi(p, t)|^2$ shown in Figs. 1 and 2. During the collision, instead of being dominated by the intrinsic width of a single $\phi(p, t)$ peak, Δp is dominated by the distance between the peaks.

From the explicit numerical calculations used to generate Fig. 5(a), we find to an excellent approximation that the position-space spread at the collision time is given by

$$\frac{\Delta x_{T_C}^{(wall)}}{\Delta x_{T_C}^{(free)}} \approx 0.60 \quad (14)$$

and we can make use of the more analytic approach followed by Andrews, at least at $t = T_C$ where the expressions simplify dramatically, to understand this effect quantitatively. Using the explicit $\psi_1(x, t)$ in Eqn. (5) and the expression in Eqn. (9), we can construct an excellent approximation to the ‘bouncing’ wave packet for the Gaussian case, namely

$$|\tilde{\psi}(x, T_C)|^2 = \frac{4}{\beta_{T_C} \sqrt{\pi}} \sin^2\left(\frac{p_0 x}{\hbar}\right) e^{-x^2/\beta_{T_C}^2} \quad (15)$$

which is approximately normalized, and the error is exponentially small for the parameters we use, namely $p_0 \beta_{T_C} / \hbar \gg 1$. For these values, the $\sin^2(p_0 x / \hbar)$ variation can very reasonably be replaced by its average value of 1/2 and the resulting integrals performed exactly. We then have, to an excellent approximation,

$$\langle x \rangle_{T_C} = -\frac{\beta_{T_C}}{\sqrt{\pi}} \quad \text{and} \quad \langle x^2 \rangle_{T_C} = \frac{\beta_{T_C}^2}{2} \quad (16)$$

so that

$$\Delta x_{T_C} = \beta_{T_C} \sqrt{\frac{1}{2} - \frac{1}{\pi}} \quad \text{or} \quad \frac{\Delta x_{T_C}^{(wall)}}{\Delta x_{T_C}^{(free)}} = \sqrt{\frac{\pi - 2}{\pi}} \approx 0.603 \quad (17)$$

all of which are observed numerically!

A similar semi-analytic result can be obtained which describes the expectation value of the momentum operator at the collision time, namely $\langle \hat{p} \rangle_{T_C}$. The values of $\langle p \rangle_t$ required for Figs. 4 and 5 have been obtained numerically, by using the momentum space probability density, but using the wavefunction representation in Eqn. (9), we can also obtain an explicit formula for $\langle \hat{p} \rangle_t$ for the special case of $t = T_C$ using the representation of \hat{p} as a differential operator acting on the position-space wavefunction. For the free-particle wave packet we naturally have

$$\langle \hat{p} \rangle_t = \int_{-\infty}^{+\infty} \psi_1(x, t)^* \hat{p} \psi_1(x, t) dx = p_0 \quad (18)$$

and the evaluation is straightforward and well-defined for all times. In contrast to this case, if we naively attempt to evaluate $\langle \tilde{\psi} | \hat{p} | \tilde{\psi} \rangle$ in this way we find that the expectation values are not necessarily Hermitian due to the ‘asymmetry’ caused by the presence of the wall. If, however, we instead adopt the ‘symmetrized’ version (which reduces to the standard value for the free-particle case)

$$\langle \hat{p} \rangle_{T_C} = \frac{1}{2} \int_{-\infty}^0 \left[\left(\hat{p} \tilde{\psi}(x, T_C) \right)^* \tilde{\psi}(x, T_C) + \tilde{\psi}^*(x, T_C) \left(\hat{p} \tilde{\psi}(x, T_C) \right) \right] dx \quad (19)$$

we find that $\langle \hat{p} \rangle$ is guaranteed to be real. Using this trick, we find that the expectation value at the collision time is

$$\begin{aligned} \langle \hat{p} \rangle_{T_C} &= - \left(\frac{4\hbar}{\sqrt{\pi}} \frac{t}{t_0} \right) \frac{1}{\beta_{T_C}^3} \left[\int_{-\infty}^0 x \sin^2 \left(\frac{p_0 x}{\hbar} \right) e^{-x^2/\beta_{T_C}^2} dx \right] \\ &\approx - \frac{1}{\alpha \sqrt{\pi}} \left[\frac{T_C/t_0}{\sqrt{1 + (T_C/t_0)^2}} \right] \end{aligned} \quad (20)$$

where $\sin^2(p_0 x/\hbar)$ term is replaced by its average value of 1/2. This analytic approximation agrees with all of our numerical calculations to the desired accuracy.

References

- [1] See, for example, Hiller J R, Johnston I D and Styer D F 1995 *Quantum Mechanics Simulations: The Consortium for Upper-Level Physics Software* (New York: Wiley).
- [2] Liboff R L 1991 *Introductory Quantum Mechanics* (Reading: Addison-Wesley) 2nd edition pp. 555-556.
- [3] Robinett R W 1995 Quantum and classical probability distributions for position and momentum Am. J. Phys. **63** 823-832.
- [4] Rowe E G Peter 1987 The classical limit of quantum mechanical hydrogenic radial distributions Eur. J. Phys. **8**, 81-87.
- [5] Robinett R W 1997 *Quantum Mechanics: Classical Results, Modern Systems, and Visualized Examples* (New York: Oxford University Press).
- [6] Goldberg A, Schey H M, and Schwartz J L 1967 Computer-generated motion pictures of one-dimensional quantum-mechanical transmission and reflection phenomena Am. J. Phys. **35** 177-186.
- [7] Bramhall M H and Casper B M 1970 Reflections on a wave packet approach to quantum mechanical barrier penetration Am. J. Phys. **38** 1136-1145.
- [8] Diu B (1980) Plane waves and wave packets in elementary quantum mechanics problems Eur. J. Phys. **1** 231-240.
- [9] Edgar A 1995 Reflection of wave packets from a quantum well with a tunneling transmission resonance Am. J. Phys. **63** 136-141.

- [10] Boleman J S and Haley S B 1975 More time-dependent calculations for the Schrödinger equation Am. J. Phys. **43** 270-271.
- [11] Greenman J V 1972 Non-dispersive mirror wave packets Am. J. Phys. **40** 1193-1201.
- [12] Segre C U and Sullivan J D 1976 Bound-state wave packets Am. J. Phys. **44** 729-732.
- [13] Deutchman P A 1971 Tunneling between two square wells – Computer movie Am. J. Phys. **39** 952-954.
- [14] Johnson E A and Williams H Thomas 1981 Quantum solutions for a symmetric double square well Am. J. Phys. **50** 239-243.
- [15] Hamilton J C, Schwartz J L, and Bowers W A 1972 Computer generated films for solid state physics Am. J. Phys. **40**, 1657-1972.
- [16] Friedmann G. and Little W A 1993 A study of a wave function of a particle striking a crystal interface , Am. J. Phys. **61**, 835-843.
- [17] Brown L S 1972 Classical Limit of the hydrogen atom Am. J. Phys. **41** 525-530.
- [18] Nauenberg M 1989 Quantum wave packets on Kepler elliptic orbits Phys. Rev. **A40** 1133-1136.
- [19] Nauenberg M, Stroud C, and Yeazell J 1994 The classical limit of an atom Sci. Am. **270** 44-49.
- [20] For a review, see Alber G and Zoller P 1991 Laser excitation of electronic wave packets in Rydberg atoms Phys. Rep **199** 231-280.

- [21] See, e.g., Press W H, Flannery B P, Teukolsky S A, and Wetterling W T *Numerical Recipes: The Art of Scientific Computing* (Cambridge: Cambridge University Press).
- [22] Blinder S M 1968 Evolution of a Gaussian wave packet Am. J. Phys. **36** 525-526.
- [23] Robinett R W 1996 Quantum mechanical time-development operator for the uniformly accelerated particle Am. J. Phys. **64** 803-808.
- [24] Merrill J R 1973 The propagation of quantum mechanical wave packets Am. J. Phys. **41** 1101-1103.
- [25] Andrews M 1998 Wave packets bouncing off walls Am. J. Phys. **66** 252-254.
- [26] See, e.g., Ref. [5] pp. 60-61.
- [27] Saxon D S 1968 *Elementary Quantum Mechanics* (New York: McGraw-Hill) pp. 144-147.
- [28] Styer D F 1989 The motion of wave packets through their expectation values and uncertainties Am. J. Phys. **58** 742-744.

Figure Captions

Fig. 1. Plots of a Gaussian wave packet striking an infinite wall (bold vertical line.)

$|\psi(x, t)|^2$ versus x is shown on the left, while the corresponding $|\phi(p, t)|^2$ versus p plot is shown on the right. The initial position x_0 is shown on the left, while the values of the central momentum long before ($+p_0$) and long after ($-p_0$) the collision are indicated on the right. The numerical values used are those in Eqn. (11).

Fig. 2. Same as Fig. 1, but for a wave packet described by an initial Lorentzian (given by Eqns. (12) and (13)) which then evolve in time.

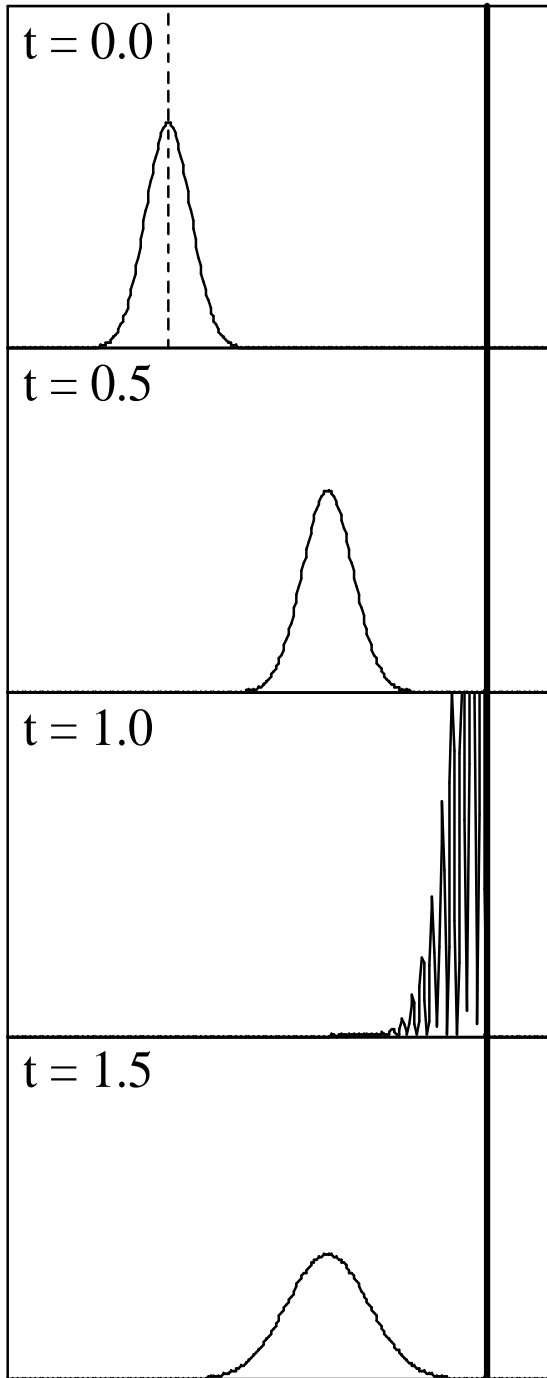
Fig. 3. Same as Fig. 1, but for times nearer the actual ‘collision’ at $t \approx T_C$. Note that the momentum distribution at the moment of collision is *not* symmetric. The peak near $+p_0$ is skewed towards values with $p \lesssim +p_0$, while the feature near $-p_0$ is similarly enhanced with values just below $-p_0$.

Fig. 4. Plot of $\langle x \rangle_t$ (top) and $\langle p \rangle_t$ (bottom) as a function of time over the same time interval as shown in Fig. 1. In order to emphasize the spreading of the wave packet, we use $\alpha = 0.5$; otherwise the parameters are as in Eqn. (11). Results are shown for the bouncing (solid curves) and the free-particle (dotted curves) packets. The dashed lines indicate the one standard deviation spreads in each case, calculated numerically. Note that the expectation value of momentum at the collision time $t = T_C$ is slightly negative.

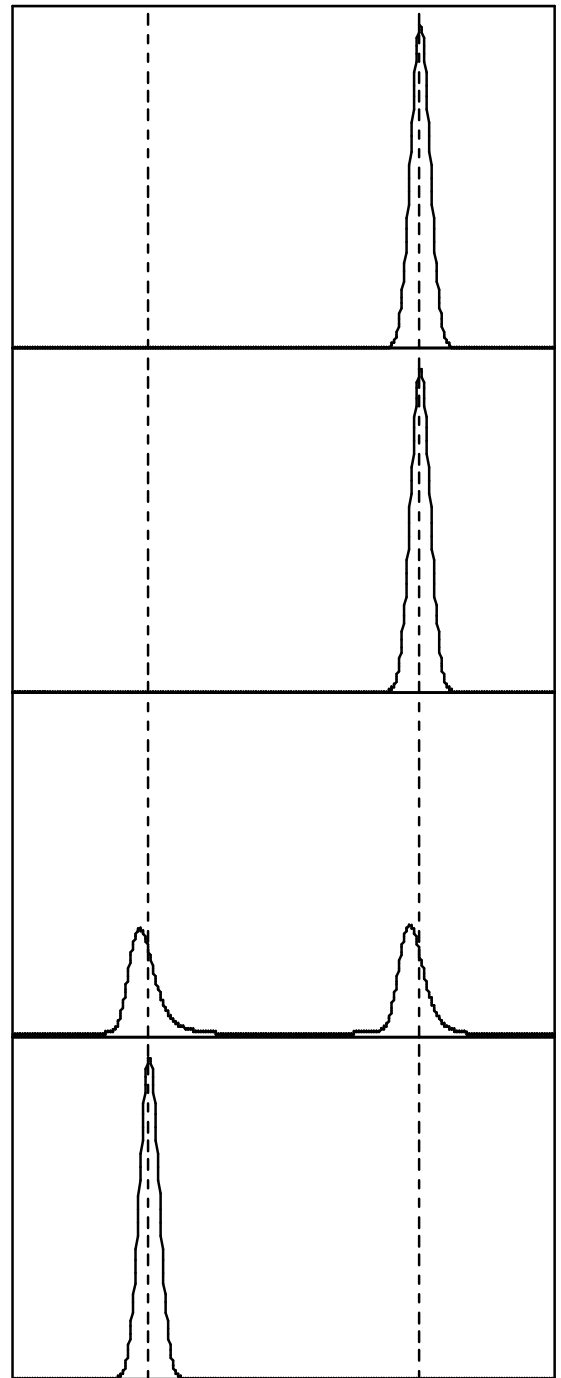
Fig. 5. Plots of (a) Δx_t , (b) Δp_t and (c) the uncertainty principle product $\Delta x_t \cdot \Delta p_t$ (in units of \hbar) versus t for various ‘bouncing’ wavepackets over the same time

interval as in Fig. 1. The various cases corresponding to $\alpha = 3, 2, 1, 1/2, 1/3$ are given by the dash-dash-dot, dash, solid, dot-dash, and dotted curves. Otherwise, the standard set of parameters in Eqn. (11) are used. All the Gaussian packets shown start with $\Delta x_t \cdot \Delta p_t = \hbar/2$.

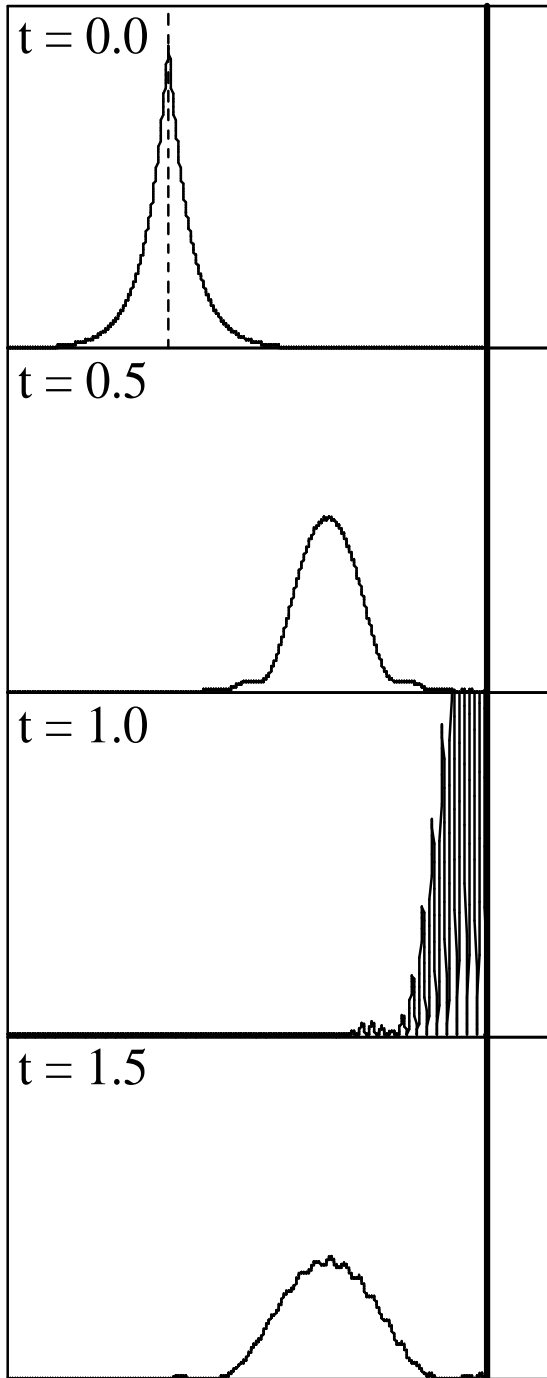
$$|\psi(x,t)|^2$$

 x_0 $x = 0$

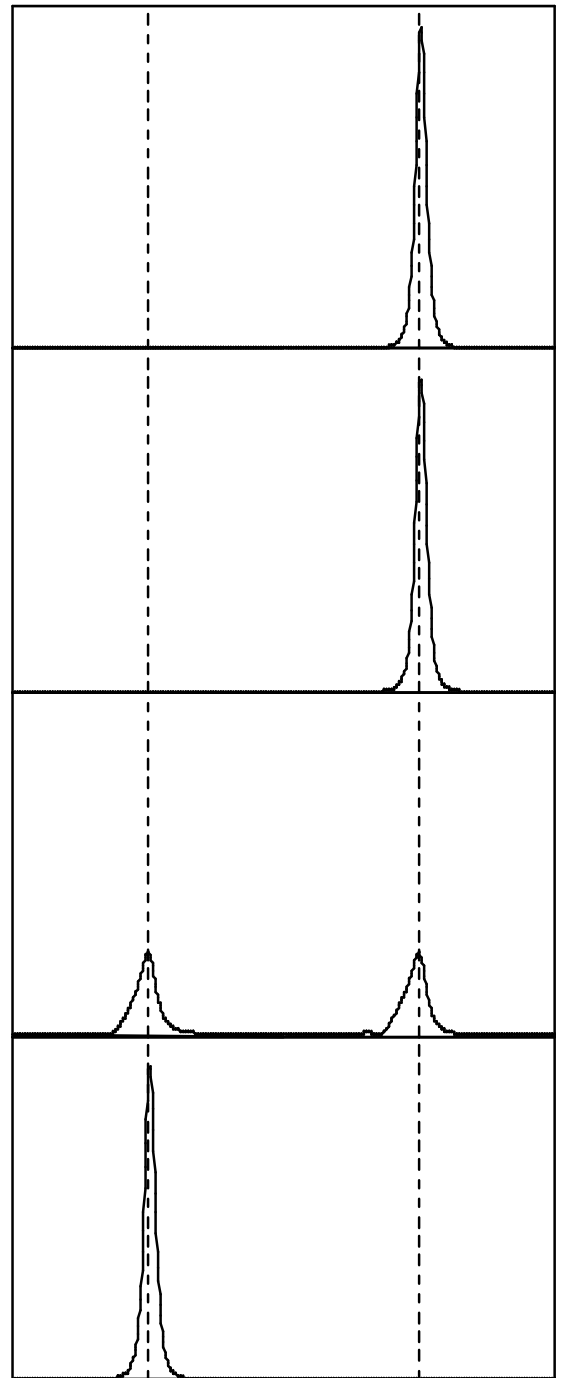
$$|\phi(p,t)|^2$$

 $-p_0$ $+p_0$

$$|\psi(x,t)|^2$$

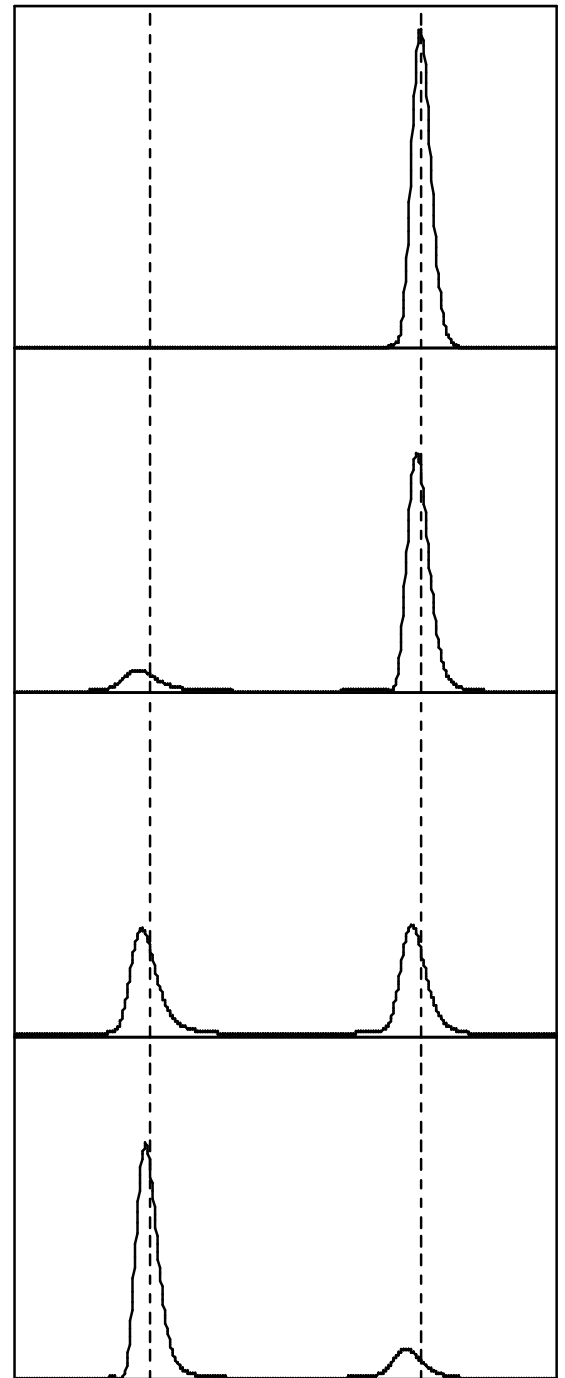
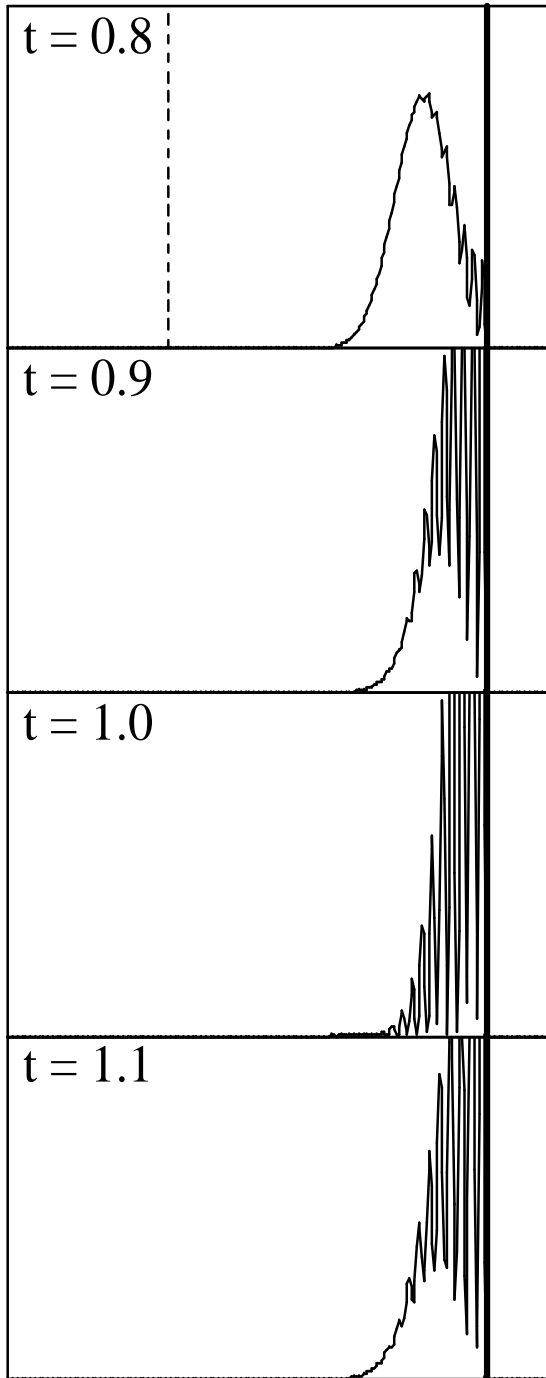
 x_0 $x = 0$

$$|\phi(p,t)|^2$$

 $-p_0$ $+p_0$

$$|\psi(x,t)|^2$$

$$|\phi(p,t)|^2$$

 x_0 $x = 0$ $-p_0$ $+p_0$

